This paper is available on line at http://www.mcponline.org

Molecular Diversity and Functional Evolution of Scorpion Potassium Channel Toxins*[S]

Shunyi Zhu‡§, Steve Peigneur¶, Bin Gao‡, Lan Luo‡, Di Jin‖, Yong Zhao‖, and Jan Tytgat¶

Scorpion toxins affecting K^+ channels (KTxs) represent important pharmacological tools and potential drug candidates. Here, we report molecular characterization of seven new KTxs in the scorpion *Mesobuthus eupeus* by cDNA cloning combined with biochemical approaches. Comparative modeling supports that all these KTxs share a conserved cysteine-stabilized α-helix/β-sheet structural motif despite the differences in protein sequence and size. We investigated functional diversification of two orthologous α-KTxs (MeuTXKα1 from *M. eupeus* and BmP01 from *Mesobuthus martensii*) by comparing their K^+ channel-blocking activities. Pharmacologically, MeuTXKα1 selectively blocked Kv1.3 channel with nanomolar affinity (IC_{50}, 2.36 ± 0.9 nM), whereas only 35% of Kv1.1 currents were inhibited at 3 μM concentration, showing more than 1271-fold selectivity for Kv1.3 over Kv1.1. This peptide displayed a weak effect on *Drosophila Shaker* channel and no activity on Kv1.2, Kv1.4, Kv1.5, Kv1.6, and human *ether-a-go-go*-related gene (hERG) K^+ channels. Although BmB01 and MeuTXKα1 have a similar channel spectrum, their affinity and selectivity for these channels largely varies. In comparison with MeuTXKα1, BmP01 only exhibits a submicromolar affinity (IC_{50}, 133.72 ± 10.98 nM) for Kv1.3, showing 57-fold less activity than MeuTXKα1. Moreover, it lacks the ability to distinguish between Kv1.1 and Kv1.3. We also found that MeuTXKα1 inhibited the proliferation of activated T cells induced by phorbol myristate acetate and ionomycin at micromolar concentrations. Our results demonstrate that accelerated evolution drives affinity variations of orthologous α-KTxs on Kv channels and indicate that MeuTXKα1 is a promising candidate to develop an immune modulation agent for human autoimmune diseases. ***Molecular & Cellular Proteomics 10: 10.1074/mcp.M110.002832, 1–11, 2011.***

Potassium (K^+) channels are a large family of membrane proteins ubiquitously distributed in both excitable and nonexcitable cells. Members in this family are involved in diverse physiological processes, including action potential repolarization, Ca^{2+} signaling, cellular proliferation and migration, and cell volume regulation (1). Some K^+ channels have been validated to be ideal targets for the development of new therapeutic drugs. For example, Kv1.3, a voltage-gated K^+ channel expressed on human effector memory T lymphocytes, is a target for the therapeutic modulation of the immune system (2). Identification and characterization of highly selective agents to modulate the functions of Kv1.3 will help develop new drugs for human autoimmune diseases.

As the oldest venomous arachnid on earth, the scorpion has evolved a large number of toxins affecting K^+ channels (called KTxs[1]) as part of its arsenal (3). According to the widely accepted nomenclature proposed by Tytgat *et al.* (4), KTxs can be further divided into four groups: α, β, γ, and κ (4–6). With the exception of the κ-KTxs that adopt a bihelical scaffold stabilized by two disulfide bridges, all other toxin groups contain a conserved α-helix/β-sheet (CS$\alpha\beta$) structural motif composed of a single α-helix and one β-sheet of two antiparallel strands (7). The α-KTx group includes short-chain peptides of 23–42 amino acids with three or four disulfide bridges and primarily affects voltage-gated *Shaker*-related and *ether-a-go-go*-related gene (ERG) K^+ channels as well as Ca^{2+}-activated K^+ channels of high, intermediate, or small conductance (8). Most peptides in this group have a functional dyad involved in the blockade of *Shaker*-related Kv channels (9). The β-KTx group contains long-chain toxins of 50–75 amino acids, which can be considered as an N-terminal extension on the α-KTx scaffold. Some examples include BmTXKβ, HgeβKTx, TcoKIK, TdiKIK, TstβKTx, and TtrKIK (10). Recombinant BmTXKβ has been confirmed to be a blocker of transient outward K^+ current (I_{to}) in rabbit atrial myocytes that is fast inactivating and associated with heteromultimeric channels with Kv4.2 and Kv4.3 subunits (11), whereas native TstβKTx is a blocker of Kv1.1 with an IC_{50} of 96 nM (10).

In this work, we report seven new KTx genes expressed in the scorpion *Mesobuthus eupeus* venom gland and their relation-

From the ‡Group of Animal Innate Immunity, State Key Laboratory of Integrated Management of Pest Insects and Rodents and ‖Transplantation Biology Research Division, State Key Laboratory of Biomembrane and Membrane Biotechnology, Institute of Zoology, Chinese Academy of Sciences, Beijing 100101, China and ¶Laboratory of Toxicology, University of Leuven, O and N 2, Postbus 922, Herestraat 49, 3000 Leuven, Belgium

Received, July 3, 2010, and in revised form, September 24, 2010
Published, MCP Papers in Press, September 30, 2010, DOI 10.1074/mcp.M110.002832

[1] The abbreviations used are: KTx, toxin affecting K^+ channels; CS$\alpha\beta$, conserved α-helix/β-sheet; hERG, human *ether-a-go-go*-related gene; PMA, phorbol myristate acetate; RP, reverse phase; IR, inactivation-removed; ChTX, charybdotoxin; Aam-KTX, *Androctonus amoreuxi* kaliotoxin; NTX, noxiustoxin.

ship with other known toxins based on sequence, structural, and evolutionary analysis. Experimental data are provided to support functional diversification between two orthologous toxins through accelerated amino acid substitutions. We found that MeuTXKα1, an orthologue of the *Mesobuthus martensii* toxin BmP01, has properties that make it an attractive candidate for development of an immune modulation agent for human autoimmune diseases with therapeutic potential. These properties include 1) high affinity on Kv1.3 (IC_{50}, 2.36 $\pm$ 0.9 nM); 2) more than 1271-fold selectivity for Kv1.3 over Kv1.1; 3) a lack of activity on Kv1.2, Kv1.4, Kv1.5, Kv1.6, and human *ether-a-go-go*-related gene (hERG) K^+ channels; and 4) inhibition of the proliferation of activated T cells induced by phorbol myristate acetate (PMA) and ionomycin.

MATERIALS AND METHODS

Construction and Screening of cDNA Library—The construction of the cDNA library from the *M. eupeus* venom gland has been described previously (12). Clones carrying an insert of 300–1000 bp potentially encoding venom peptide precursors were selected for DNA sequencing by primer T25V. Nucleotide sequences reported here have been deposited in the GenBank™ database (http://www.ncbi.nlm.nih.gov) under accession numbers EF442060 (*MeuTXKα1*), EF445085 (*MeuTXKα2*), EF442052 (*MeuTXKα3*), EF442053 (the long transcript of *MeuTXKα3*), EF445083 (*MeuTXKα4*), EF442047 (*MeuTXKβ3*), EF445099 (*MeuTXKβ4*), and EF445076 (*MeuTXKβ5*).

Bioinformatics Identification of New Potassium Channel Toxins—A similarity search of the GenBank database (GenBank release 177.0) by BLASTP (BLAST 2.2.23) was used to find homologues of new *M. eupeus* venom peptides. Protein sequences were aligned by ClustalX 1.83 (http://www.ebi.ac.uk). Phylogenetic trees reported here were reconstructed from the alignments by MEGA 4.0 (http://www.megasoftware.net/mega.html), and they are all bootstrap consensus trees based upon 1000 replications of the neighbor-joining algorithm with Poisson correction. Numbers on the branches are bootstrap percentages. Three-dimensional structures of all the toxins described here were built by comparative modeling at SWISS-MODEL, a fully automated protein structure homology-modeling server (http://swissmodel.expasy.org/), except MeuTXKβ5-NHD(S) that was predicted by an *ab initio* modeling method on the I-TASSER server (http://zhanglab.ccmb.med.umich.edu/I-TASSER/) because of the lack of a suitable template for its extended N terminus. In the comparative modeling, aligned sequences of the target and template were applied to build models through the "Alignment Mode" option, and the model quality was evaluated by Verify3D. Structural superimposition was performed using MultiProt (http://bioinfo3d.cs.tau.ac.il/MultiProt/) to identify a conserved functional motif. MOLMOL (molmol-2k.2.0) (13) was used to display, analyze, and manipulate toxin structures in which electrostatic potentials mapped on the model structure surface were calculated by the "simplecharge" command, and blue and red surface areas indicate positive and negative charges, respectively.

Isolation and Purification of MeuTXKα1 and BmP01—Purification approaches used here have been described previously (14). Briefly, *M. eupeus* or *M. martensii* (previously called *Buthus martensii* (15)) crude venoms collected by an electrical stimulation method were resuspended in 0.1% trifluoroacetic acid (TFA; v/v) and directly subjected to RP-HPLC isolation. The Agilent Zorbax 300SB-C_{18} (4.6 $\times$ 150 mm, 5 μm) was equilibrated with 0.1% TFA in water (v/v), and peptide components were eluted from the column with a linear gradient from 0 to 60% acetonitrile in 0.1% TFA in water (v/v) within 60 min with a flow rate of 1 ml/min. The UV absorbance trace was followed at 225 nm. All well defined peaks were separately collected and rerun on the same column to purify these peptides further. The purity of MeuTXKα1 and BmP01 was identified by MALDI-TOF and Edman degradation, which determines their N-terminal sequences. The amino acid sequence of MeuTXKα1 has been deposited in the UniProtKB protein database (http://www.ebi.ac.uk/uniprot/) under the accession number P86400.

Expression in Xenopus Oocytes—For the expression of the voltage-gated K^+ channels (rKv1.1, rKv1.2, rKv1.3, hKv1.3, rKv1.4, rKv1.5, rKv1.6, *Shaker* IR, and hERG) in *Xenopus* oocytes, the linearized plasmids were transcribed using the T7 or SP6 mMESSAGE-mMACHINE transcription kit (Ambion) (supplemental Table S1). The harvesting of stage V-VI oocytes from an anesthetized female *Xenopus laevis* frog was as described previously (16). Oocytes were injected with 50 nl of cRNA at a concentration of 1 ng/nl using a microinjector (Drummond Scientific). The oocytes were incubated in a solution containing 96 mM NaCl, 2 mM KCl, 1.8 mM $CaCl_2$, 2 mM $MgCl_2$, and 5 mM HEPES (pH 7.4) supplemented with 50 mg/liter gentamycin sulfate.

Electrophysiological Recordings—Two-electrode voltage clamp recordings were performed at room temperature (18–22 °C) using a Geneclamp 500 amplifier (Axon Instruments) controlled by a pCLAMP data acquisition system (Axon Instruments). Whole-cell currents from oocytes were recorded 4–5 days after injection. Bath solution composition was 96 mM NaCl, 2 mM KCl, 1.8 mM $CaCl_2$, 2 mM $MgCl_2$, and 5 mM HEPES (pH 7.4). Voltage and current electrodes were filled with 3 M KCl. Resistances of both electrodes were kept as low as possible ($<$1.0 megaohm). The elicited currents were filtered at 1 kHz and sampled at 2 kHz using a four-pole low pass Bessel filter. Leak subtraction was performed using a P/4 protocol. Kv1.1–Kv1.6 and *Shaker* currents were evoked by 500-ms depolarizations to 0 mV followed by a 500-ms pulse to $-$50 mV from a holding potential of $-$90 mV. Current traces of hERG channels were elicited by applying a +40-mV prepulse for 2 s followed by a step to $-$120 mV for 2 s. To assess the concentration dependence of the MeuTXKα1-induced inhibitory effects, dose-response curves were constructed. The percentage of blocked current was plotted as a function of increasing toxin concentrations. Each experiment was performed at least 3 times ($n \geq 3$). All data are presented as means $\pm$ S.E.

Proliferation Assay of T Cells on PMA/Ionomycin—C57BL/6 mice (6 weeks old, male) were purchased from Beijing Laboratory Animal Research Center (Beijing, China). All mice were maintained in a specific pathogen-free facility and were housed in microisolator cages containing sterilized feed, autoclaved bedding, and water. Single cell suspensions were prepared by grinding the spleen tissues with the plunger of a 5-ml disposable syringe and were then suspended in RPMI 1640 medium. Splenocytes were treated with a hemolytic buffer (17 mM Tris-HCl and 140 mM NH_4Cl (pH 7.2)) to remove red blood cells as described before (17).

Splenocytes (2×10^5cells/well) were cultured in a flat bottom plate pretreated with various concentrations of toxin for 1 h before addition of 10 ng/ml PMA and 1 μM ionomycin for 72 h at 37 °C in 5% CO_2. 0.4 μCi of [^{3}H]thymidine (185 GBq/mmol) was added to each well for the last 12 h. Cells were harvested onto glass fiber filters with an automatic cell harvester (Tomtec, Toku, Finland). Samples were assayed in a Liquid Scintillation Analyzer (Beckman Instruments). Values are presented as counts per minute (cpm) of triplicate wells.

Construction of Structure Model of MeuTXKα1/BmP01 and Kv1.3—The initial complex model of MeuTXKα1/BmP01 and human Kv1.3 was constructed by replacing the coordinate of Css20 in the Css20-hKv1.3 complex constructed by Rodríguez de la Vega and co-workers (18) using the structures of MeuTXKα1/BmP01 based on their toxin structural similarity. To relieve steric clashes in the initial model, we performed energy minimization using the DeepView pro-

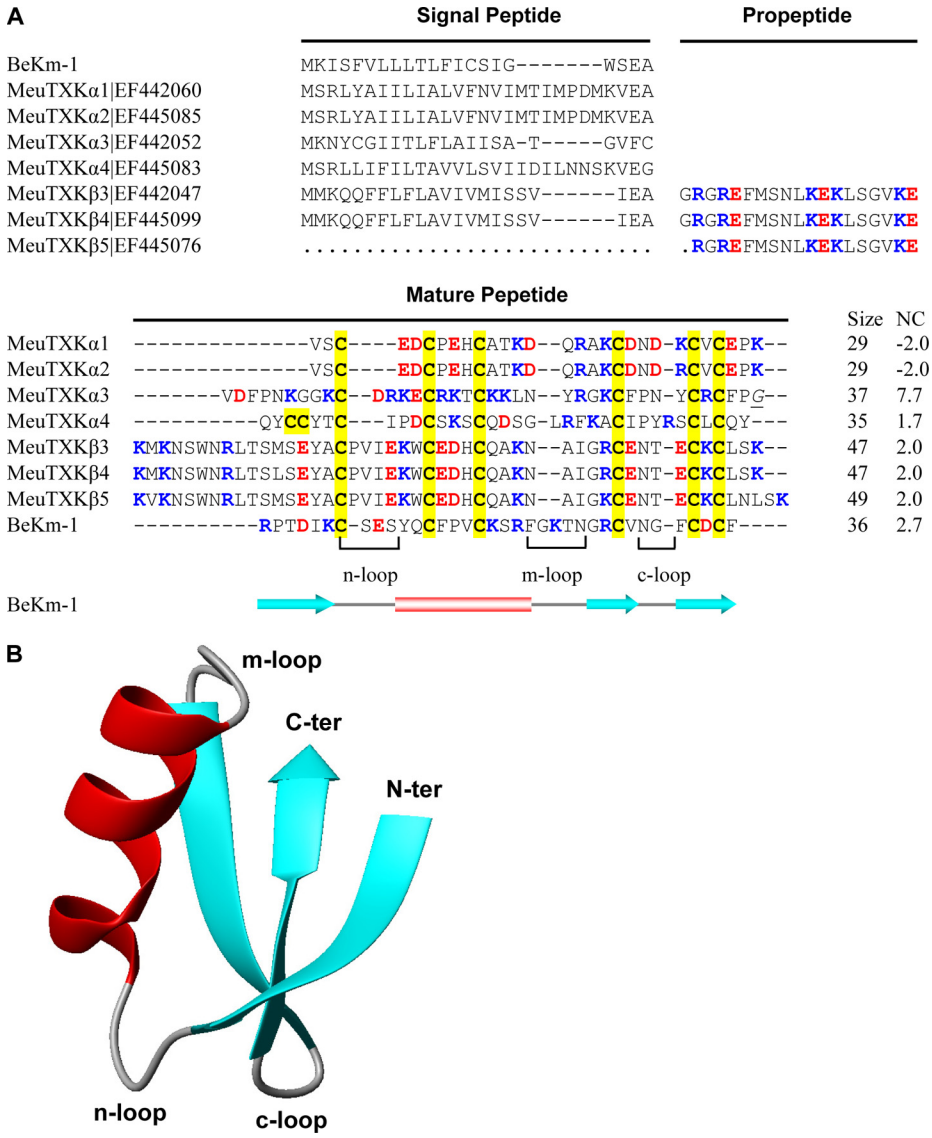

FIG. 1. ***M. eupeus* KTxs.** *A*, sequence alignment of protein precursors. Gaps were introduced to improve the alignment, and *dots* represent residues not determined because of an incomplete cDNA sequence. Cysteines are shadowed in *yellow*. Acidic and basic residues are shown in *red* and *blue*, respectively. The *italicized* and *underlined* glycine in MeuTXKα3 is presumably removed during post-translational processing. Net charge (*NC*) was calculated at pH 7.0 using Protein Calculator v3.3 (http://www.scripps.edu/~cdputnam/protcalc.html). Secondary structure elements of BeKm-1 were extracted from its experimental structure (Protein Data Bank code 1J5J) by STRIDE (http://webclu.bio.wzw.tum.de/stride/). *B*, MOLMOL figure showing the ribbon structure of BeKm-1.

gram (Swiss-PDB Viewer, http://www.expasy.ch/spdv/). Only the BmP01-hKv1.3 complex model was further analyzed in detail.

RESULTS

Isolation and Characterization of M. eupeus K^+ Channel Toxin Transcripts—From the cDNA library prepared from *M. eupeus* venom glands, we isolated and identified new transcripts encoding precursors of seven KTx-like peptides (Fig. 1*A*). According to their sequence and structural features, we named these peptides MeuTXKα1, MeuTXKα2, MeuTXKα3, MeuTXKα4, MeuTXKβ3, MeuTXKβ4, and MeuTXKβ5. Of them, MeuTXKα1–4 belong to the α-KTx subfamily, and MeuTXKβ3–5 are classified into the β-KTx subfamily. Except the incomplete MeuTXKβ5 transcript (due to RNA degradation in its 5′-end), all these new KTx precursors contain a typical signal peptide as predicted by SignalP 3.0 (http://www.cbs.dtu.dk/services/SignalP/). The mature toxins are composed of 29–49 amino acids with extensive amino acid variations; however, they all contain six cysteines with an alignment pattern similar to that of known KTxs (8), indicating they may adopt a typical CSαβ folding. Structural analysis revealed that several indel mutations in *Mesobuthus* K^+ channel toxins are primarily located in three loops (Fig. 1*B*). Overall, most of these new toxin-like peptides are cationic due to the presence of 1.7–7.7 net positive charges.

New Members of α-KTx8 Subfamily—The α-KTx8 subfamily is composed of five highly similar members (α-8.1–α-8.5), including AmP01, BmP01, LpII, LpIII, and OdK-1 (Fig. 2, *A* and *B*) (19–22). MeuTXKα1 (α-8.6) and MeuTXKα2 (α-8.7) are two new α-KTx8 peptides with only one residue change (Fig. 2*A*). They both are characterized as the orthologous toxins of *M. martensii* BmP01, a non-toxic component with weak activity against SK_{Ca} channels (19). These two peptides differ from other subfamily members by at least five amino acids of which three are located on the turn linking the α-helix and the first β-strand, a key region

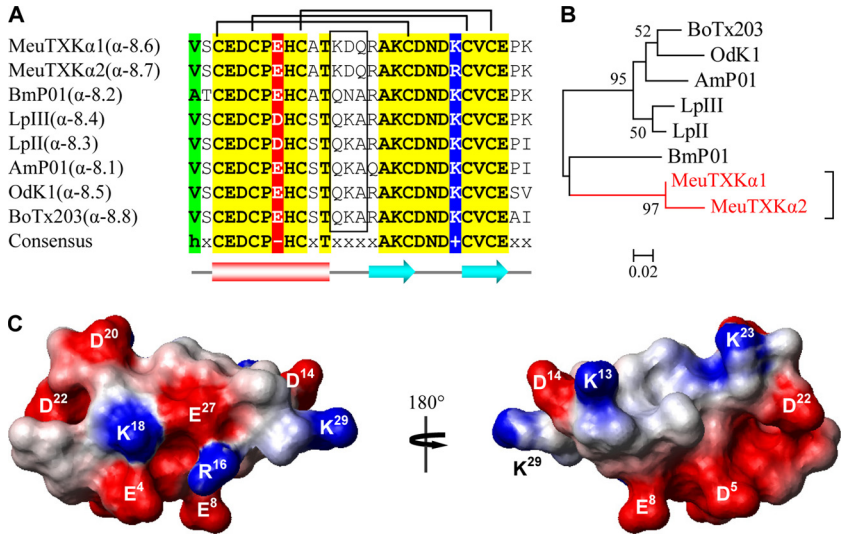

FIG. 2. **Subfamily 8 of KTxs.** *A*, multiple sequence alignment. Divergent sequences between MeuTXKα1/2 and other toxins are *boxed*. *B*, phylogeny. Only bootstrap percentages >50 are shown here. The *scale bar* shows total amino acid divergence. *C*, electrostatic potential map of MeuTXKα1 whose structure was built based on BmP01 (Protein Data Bank code 1WM7).

characterized to be important in interacting with Kv channels. There is a lysine at position 18 that is conserved across the subfamily (Fig. 2*A*). Such a lysine has been thought to be the most crucial amino acid for Kv channel blockade in many α-KTxs (8), and in some cases, a hydrophobic moiety (normally Phe or Tyr) at a distance of ~6–7 Å is also needed to form a functional dyad (9).

Comparative modeling confirms that the overall fold of MeuTXKα1 is very similar to that of BmP01, which is composed of an α-helical region spanning residues 3–12 and two strands of β-sheet spanning residues 16–19 and 24–27. The electrostatic potential of MeuTXKα1, calculated by MOLMOL, was characterized by a large negative zone around Glu^4, Asp^5, Glu^8, and Asp^{22} and a small positively charged zone composed of Lys^{13} and Lys^{23} (Fig. 2*C*).

MeuTXKα3: a Novel Toxin-like Peptide with Typical Dyad Motif and Cationic Surface—The precursor of MeuTXKα3 contains 60 amino acids, including an N-terminal signal peptide of 22 residues, a mature peptide of 37 residues, and an extra C-terminal Gly that could be removed in post-translational processing to form an amidated peptide as observed in two bee toxins, apamin and mellitin (23, 24). MeuTXKα3 is a novel toxin-like peptide with very low sequence similarity to KTxs characterized so far (Fig. 3, *A* and *B*). However, this peptide has typical structural residues for the formation of CSαβ folding, which include six cysteines and one glycine in the GKC motif (7).

The structural model of MeuTXKα3 provides evidence supporting its possible K^+ channel-blocking function. 1) As predicted from its +7.7 net charges, this molecule possesses a rather large positively charged molecular surface around Arg^{12}, Lys^{13}, Arg^{16}, Arg^{25}, Lys^{27}, and Arg^{34}. On the opposed surface of this molecule, there is a small positively charged zone composed of three lysines at sites 17, 21, and 22 (Fig. 3*C*). 2) A dyad comprising Lys^{27} and Phe^{36} can be well superimposed with that of charybdotoxin (ChTX), a well characterized scorpion α-KTx isolated from the venom of *Leiurus quinquestriatus* (7), at an ideal distance of 6.32 Å between the lysine Cα atom to the center of the aromatic ring of Phe^{36} (Fig. 3*D*).

MeuTXKα4: a Novel Toxin-like Peptide with Double Cysteine in Its N Terminus—The precursor of MeuTXKα4 is composed of 63 residues with an N-terminal signal peptide of 28 amino acids that shares 64% similarity to that of BmK86 (25), a newly characterized toxin targeting Kv1.3 from *M. martensii* (Fig. 4*A*). Overall, mature MeuTXKα4 represents a novel peptide with low sequence similarity to several toxins from the α-KTx3 subfamily and BmK86 (Fig. 4, *B* and *C*); however, it has six cysteines with an alignment pattern similar to that of other known KTxs, which could make it fold into a CSαβ structure, as confirmed by comparative modeling (Fig. 4*D*). Electrostatic potential analysis demonstrates that this peptide has a large positive zone around Arg^{21}, Lys^{23}, and Arg^{29} (Fig. 4*D*).

BmTXKβ-related Peptides—MeuTXKβ3–MeuTXKβ5 are three highly similar peptides with 30–80% sequence identity to BmTXKβ and related toxins (Fig. 5, *A* and *B*). After the signal peptide is removed, a mature peptide of 66–68 residues can be released. Considering their high degree of sequence similarity to TcoKIK (10), we hypothesized that these peptide precursors may also have an additional processing pattern to remove an N-terminal 19 residues after the signal peptide. Because there is no suitable template to build the full-length structures of these molecules by comparative modeling, computational *ab initio* prediction was chosen as an alternative, and it suggests that these peptides adopt a two-domain architecture as previously proposed in the βSPN family of scorpion venom-derived antimicrobial peptides (14, 26) in which the N-terminal part is cysteine-free and can form an α-helical conformation, whereas the C-terminal part is a typical CSαβ fold (Fig. 5*C*), consistent with the model structure of the C-terminal part obtained by comparative modeling based on the scyllatoxin structure (Protein Data Bank code 1SCY) (Fig. 5*D*). Interest-

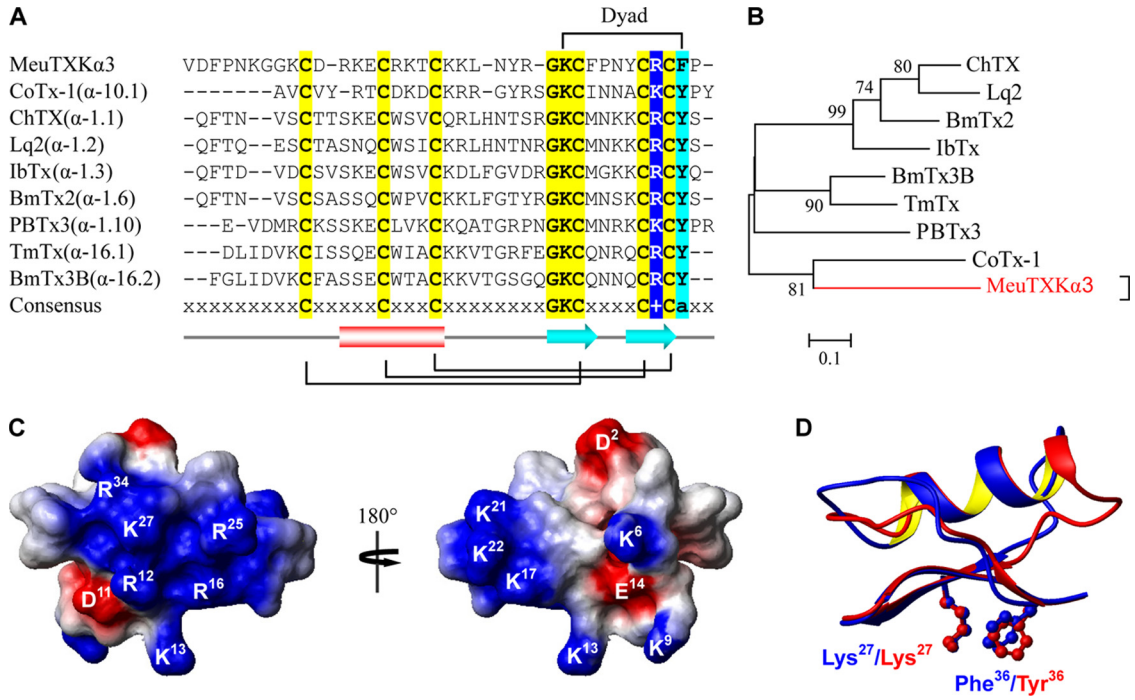

FIG. 3. **MeuTXKα3 and related KTxs.** *A*, multiple sequence alignment. The dyad residues are indicated at the *top*. *B*, phylogeny. *C*, electrostatic potential map of MeuTXKα3 whose structure was built based on ChTX (Protein Data Bank code 2CRD). *D*, structural superimposition of MeuTXKα3 and ChTX with the dyad shown in *ball-stick* models. *IbTx*, iberiotoxin; *TmTx*, tamulotoxin.

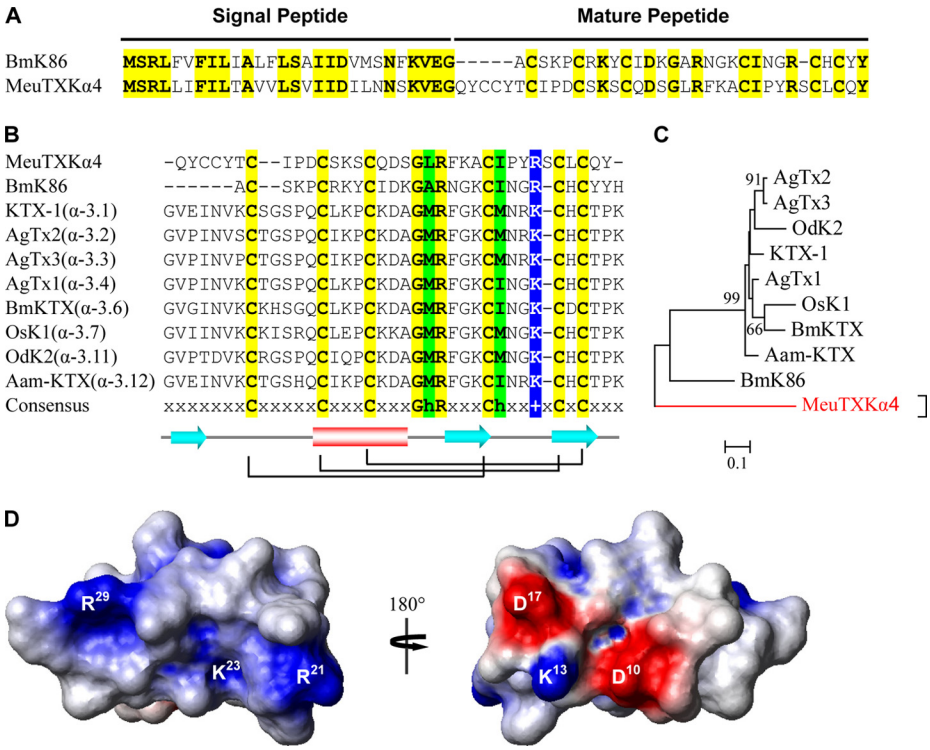

FIG. 4. **MeuTXKα4 and related KTxs.** *A*, comparison of precursor sequences of MeuTXKα4 and BmK86. *B*, multiple sequence alignment. *C*, phylogeny. *D*, electrostatic potential map of MeuTXKα4 whose structure was built based on OsK-1 (Protein Data Bank code 1SCO).

ingly, a dyad motif can be recognized in the structure of the C terminus of MeuTXKβ5 in which a conserved Lys at site 22 and a hydrophobic residue Leu at site 31 can be well superimposed with that of ChTX (Fig. 5*E*).

Biochemical Characterization and Functional Evaluation of MeuTXKα1 and BmP01—MeuTXKα1 and BmP01 are two orthologous toxins with accelerated amino acid substitutions as identified by a higher substitution rate in nonsynonymous

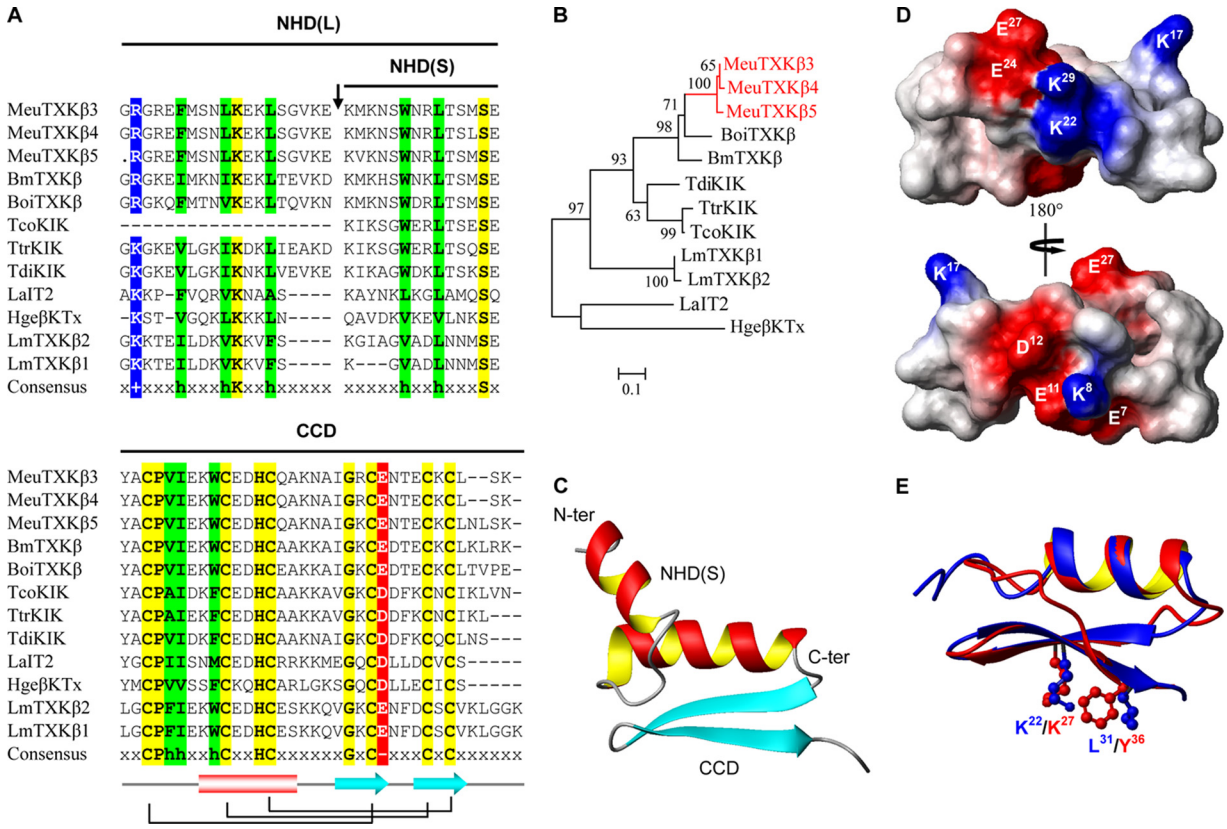

FIG. 5. **BmTXKβ-related toxins.** *A*, multiple sequence alignment. Identical residues are shadowed in *yellow*, and conservative replacements are in *red* for acidic residues, *green* for hydrophobic residues, and *blue* for basic residues. *NHD(L)*, long N-terminal helical domain; *NHD(S)*, short N-terminal helical domain; *CCD*, C-terminal CS$\alpha\beta$ domain. *B*, phylogeny. *C*, overall folding of MeuTXKβ5 short N-terminal helical domain. *D*, electrostatic potential map of the MeuTXKβ5 C-terminal CS$\alpha\beta$ domain whose structure was built based on scyllatoxin (Protein Data Bank code 1SCY). *E*, structural superimposition of the MeuTXKβ5 C-terminal CS$\alpha\beta$ domain and ChTX with the dyad shown in *ball-stick* models.

sites of the mature peptide-coding region than in those of the signal peptide-coding region (supplemental Fig. S1). To study the functional significance of the accelerated substitutions, we compared their channel-blocking activities. First, we purified MeuTXKα1 from the *M. eupeus* venom by RP-HPLC and characterized it by MALDI-TOF and Edman degradation. MeuTXKα1 was eluted at 17.5 min (Fig. 6*A*), and the molecular mass detected is 3251 Da, which accurately matches the molecular mass predicted from its amino acid sequence (3250 Da) (Fig. 6*B*). Edman degradation determined the N-terminal first five residues of the purified component, which was VSCED, completely consistent with that of MeuTXKα1 determined by cDNA cloning. By using the same approaches, we also purified BmP01 from the *M. martensii* venom (Fig. 6, *C* and *D*).

Pharmacological functions of MeuTXKα1 and BmP01 were evaluated on a panel of nine voltage-gated K$^+$ channels (rKv1.1, rKv1.2, rKv1.3, hKv1.3, rKv1.4, rKv1.5, rKv1.6, *Shaker* IR, and hERG). All channels were expressed in *Xenopus* oocytes, and their currents were recorded by using a two-electrode voltage clamp technique. Fig. 7 shows the blocking effects of MeuTXKα1 on different K$^+$ currents. At 3 μM concentration, MeuTXKα1 inhibited about 35, 100, and 70% of the peak currents of rKv1.1, hKv1.3, and *Shaker* IR channels, respectively. At this concentration, rKv1.2, rKv1.4, rKv1.5, rKv1.6, and hERG channels were not affected. For comparison, we also in parallel evaluated Kv channel-blocking activity of BmP01 on the same channels. The results showed that it exhibited a channel spectrum identical to that of MeuTXKα1 but was more potent on rKv1.1 than MeuTXKα1 because at 3 μM concentration BmP01 inhibited 100% of rKv1.1 currents (Fig. 8).

Subsequently, we compared the affinity of MeuTXKα1 and BmP01 on hKv1.3. The results demonstrated that MeuTXKα1 is a highly potent hKv1.3 channel blocker with nanomolar affinity (IC_{50}, 2.36 $\pm$ 0.9 nM) (Fig. 9), showing more than 1271-fold selectivity for Kv1.3 over Kv1.1, whereas BmP01 only exhibits a submicromolar affinity for hKv1.3 (IC_{50}, 133.72 $\pm$ 10.98 nM) and rKv1.3 (IC_{50}, 467.68 $\pm$ 28.37 nM) (Fig. 9). Overall, BmP01 shows 57-fold less activity on hKv1.3 than MeuTXKα1. Variations in affinity and selectivity for these two orthologous toxins support their functional evolution after speciation.

Given the selective potency of MeuTXKα1 on the Kv1.3 channel, we thus assayed its potential ability in inhibiting T cell proliferation mediated by the expression of Kv1.3. The results showed that MeuTXKα1 inhibited the proliferation of activated T cells induced by PMA and ionomycin in a dose-dependent manner (Fig. 10).

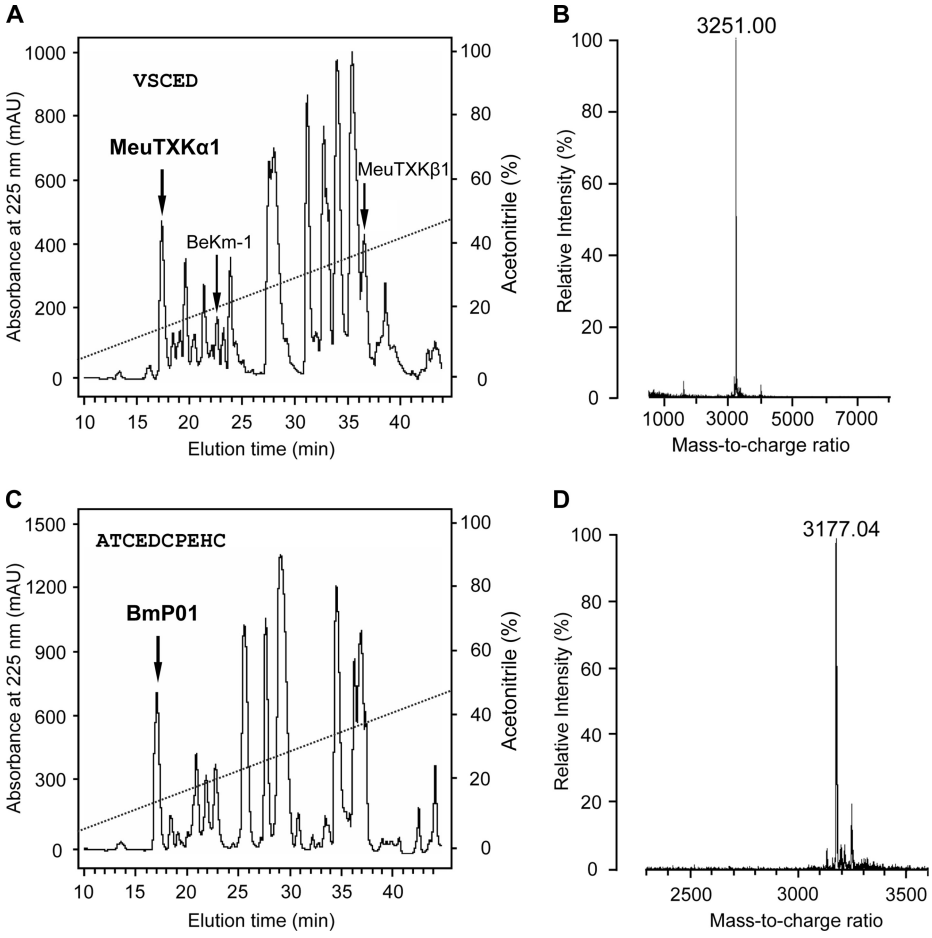

FIG. 6. **Purification and characterization of MeuTXKα1 and BmP01.** RP-HPLC analysis shows the separation of the crude venom of *M. eupeus* (*A*) and *M. martensii* (*C*) where MeuTXKα1 and BmP01 were eluted, respectively, at 17.5 and 17 min (indicated by an *arrow*). MALDI-TOF of MeuTXKα1 (*B*) and BmP01 (*D*) is shown. *mAU*, milliabsorbance units.

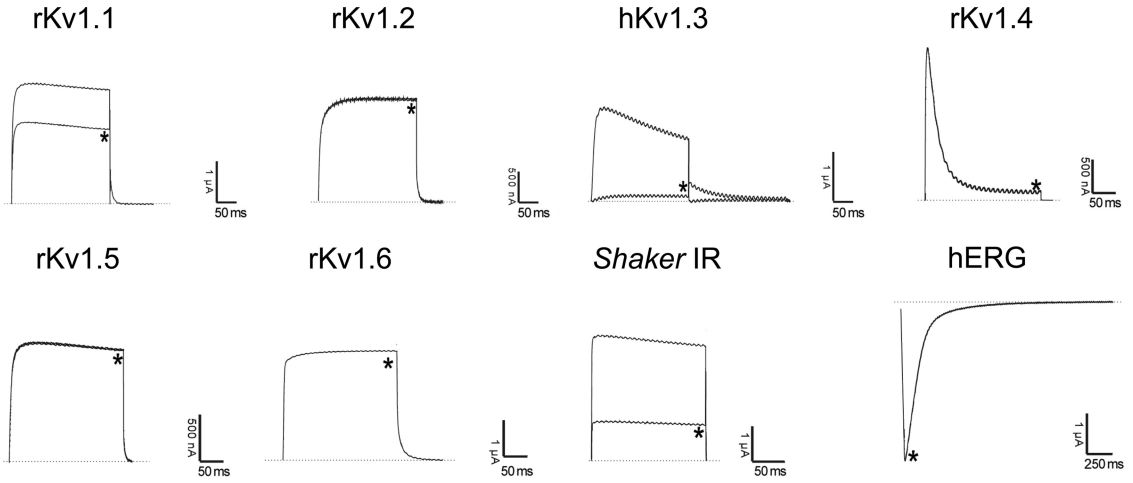

FIG. 7. **Differential effects of MeuTXKα1 on Kv channel isoforms expressed in *X. laevis* oocytes.** Representative whole-cell currents of oocytes expressing cloned Kv channels (Kv1.1–Kv1.6, hERG, and *Shaker* IR) are shown. The *dotted line* indicates the zero current level. * marks steady state current traces after administering 3 μM MeuTXKα1.

DISCUSSION

M. eupeus is a sibling species of the most widely studied species *M. martensii* (15); however, its KTxs are little known. One such peptide previously isolated from this scorpion is BeKm-1, a hERG-specific toxin, which shares structural similarity to ChTX but has a mechanism of action similar to that of ergtoxin, a member of the scorpion venom-derived γ-KTx family (27). Another KTx in this species (named MeuKTX) was recently identified as a non-selective inhibitor of Kv channels (28). To search for new KTxs from the venom of *M. eupeus*, we

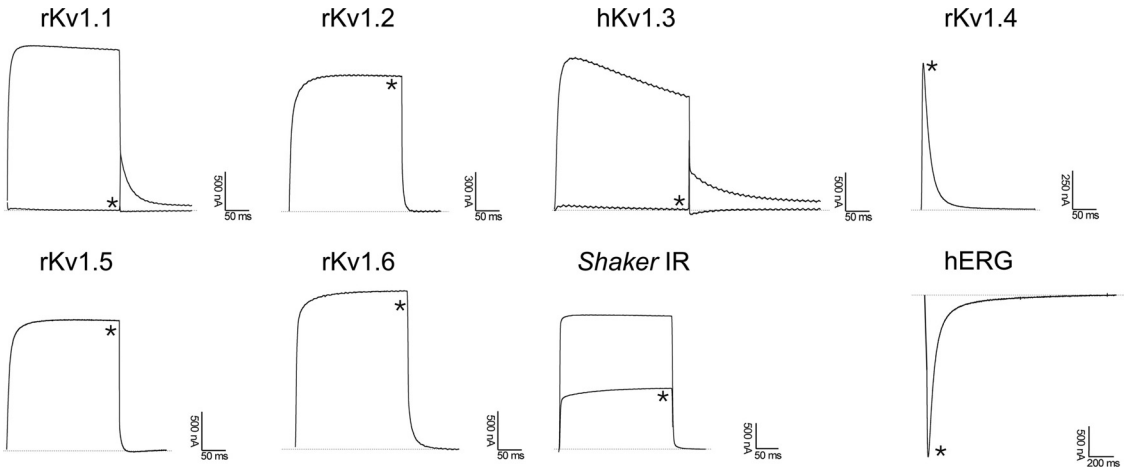

FIG. 8. **Differential effects of BmP01 on Kv channel isoforms expressed in *X. laevis* oocytes.** Representative whole-cell currents of oocytes expressing cloned Kv channels (Kv1.1-Kv1.6, hERG, and *Shaker* IR) are shown. The *dotted line* indicates the zero current level. * marks steady state current traces after administering 3 μM MeuTXKα1.

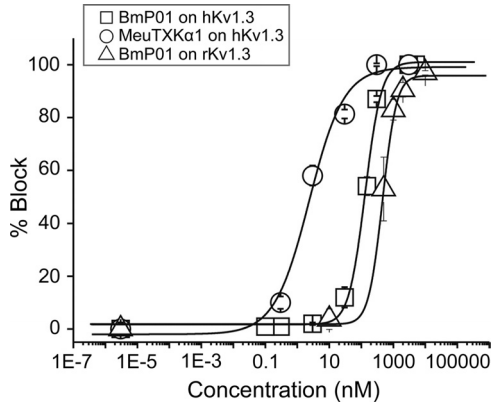

FIG. 9. **Concentration dependence of Kv1.3 current block by MeuTXKα1 and BmP01.** The yielded IC_{50} values were 2.36 $\pm$ 0.90 nM for MeuTXKα1 on hKv1.3, 133.72 $\pm$ 10.98 nM for BmP01 on hKv1.3, and 467.68 $\pm$ 28.37 nM for BmP01 on rKv1.3.

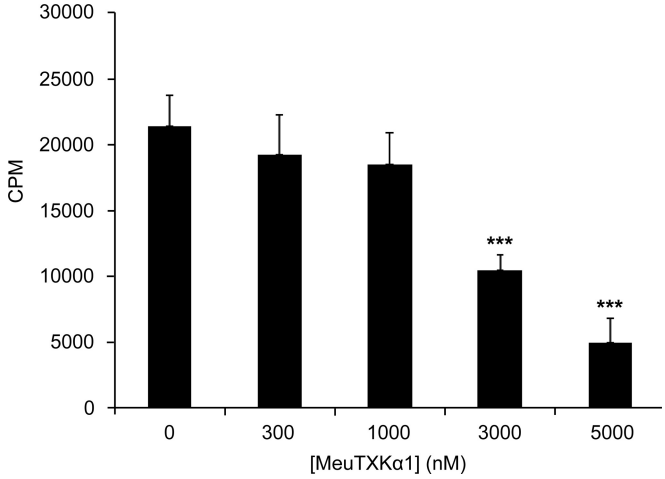

FIG. 10. **MeuTXKα1 inhibited proliferation of T cells induced by PMA/ionomycin.** Data are shown as mean $\pm$ S.D. (n = 3). Student's unpaired t test for comparison of means was used to compare groups. ***, $p < 0.001$ (compared with the control without peptides added).

TABLE I

Comparison of IC_{50} values (nM) of scorpion α-KTxs and analogues on Kv1.3 and Kv1.1 channels

Data sources are as follows: MeuTXKα1 (this work); ChTX, Mokatoxin-1, AgTx-2, and KTX (33); Aam-KTX (35); HsTx1 (34); ADWX-1 (30); AgTx-1 (39); NTX (40); OsK-1 (31); OdK-2 (32); Css20 (18); MeuKTX (28); maurotoxin (MTX) (41).

Toxin	α-KTx	Kv1.3	Kv1.1	$IC_{50(Kv1.1)}/IC_{50(Kv1.3)}$
MeuTXKα1	8.6	2.36	>3000	>1271
ChTX	1.1	0.9	>1000	>1111
Mokatoxin-1	Designed	1	>1000	>1000
Aam-KTX	3.12	1.1	>750	>682
HsTx1	6.3	0.011	7	636
ADWX-1	Designed	~0.002	0.65	340
KTX	3.1	0.01	1.1	110
AgTx-1	3.4	1.7	136	80
NTX	2.1	0.31	24	77
OsK-1	3.7	0.014	0.6	43
OdK-2	3.11	7.2	>35	>4.9
AgTx-2	3.2	0.05	0.13	2.6
Css20	2.13	7.2	>10	>1.4
MeuKTX	3.13	0.17	0.20	1.2
MTX	2.2	150	37	>0.6

first constructed a cDNA library from its venom gland from which we identified clones encoding seven putative KTxs using a random DNA sequencing strategy. Of them, five are classified as the orthologues of two known *M. martensii* toxins, including MeuTXKα1, MeuTXKα2, MeuTXKβ3, MeuTXKβ4, and MeuTXKβ5, and two (MeuTXKα3 and MeuTXKα4) share low sequence similarity to described peptides.

It is estimated that there are about 1500 known species of scorpions in the world, and each different species has around 70 peptides (3). Our work presented here indicates that even between two sibling species their orthologous toxins may have adaptively evolved new functions with differential affinity and selectivity on given K^+ channels. This supports the notion that the venom of each species should be fully evaluated in terms of their pharmacological functions (29). BmP01 and MeuTXKα1

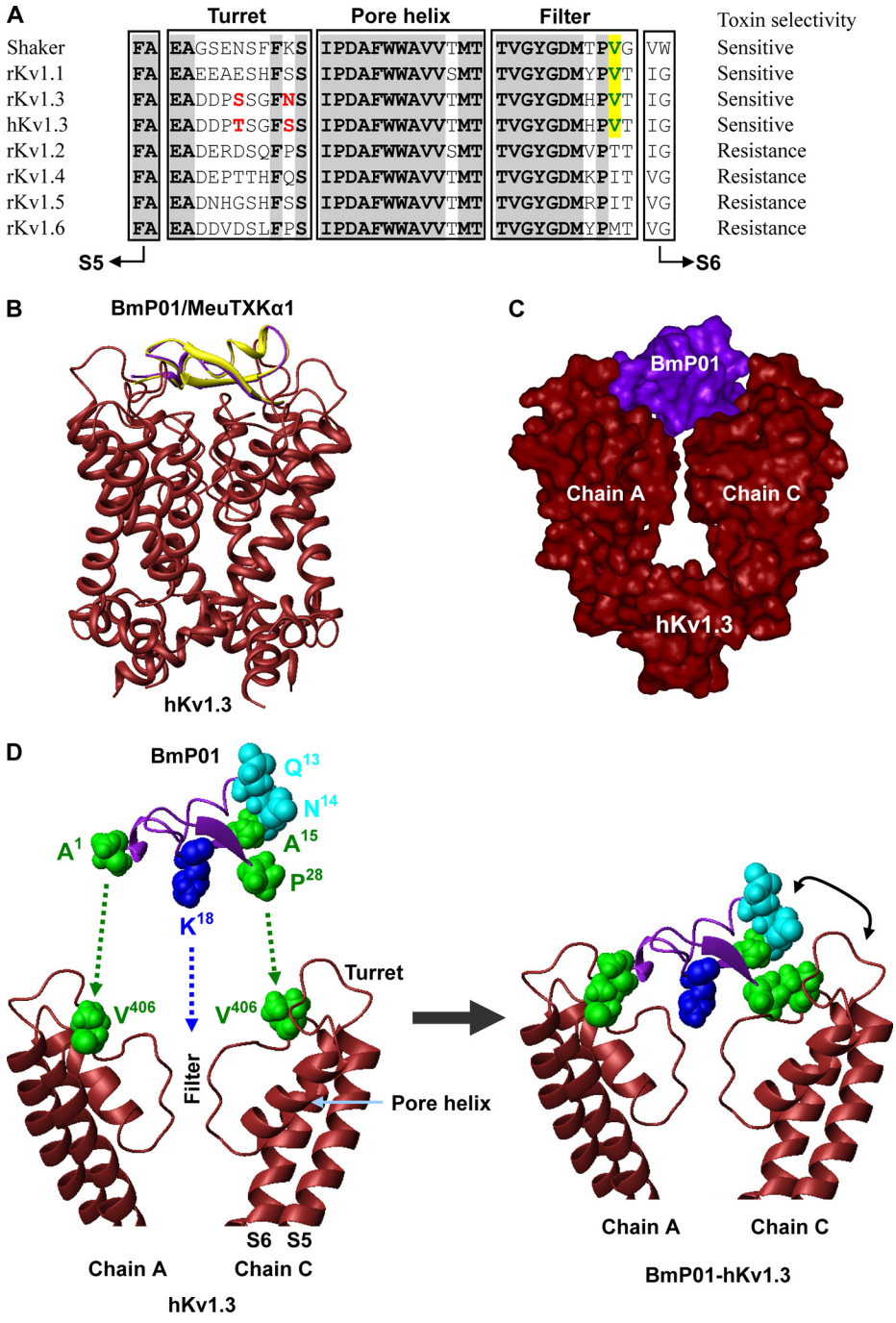

FIG. 11. **Hypothesized model for explanation of selective Kv channel-blocking activity of MeuTXKα1/BmP01.** *A*, sequence alignment of the pore region of Kv1.1–Kv1.6 and *Drosophila Shaker* channels. Val^{406}, which is conserved among sensitive Kv channels, is shown in *green* and shadowed in *yellow*. Residues that are different between rat and human Kv1.3 are in *red*. *B*, ribbon model of MeuTXKα1/BmP01 binding to human Kv1.3. *Yellow*, BmP01; *lavender*, MeuTXKα1. *C*, molecular surface representation of BmP01-hKv1.3 complex. For clarity, only chains A and C of Kv1.3 are shown here. *D*, BmP01 binds to the outer vestibule of Kv1.3 by Lys^{18} plugging into the channel pore and two hydrophobic residues (Ala^1 and Pro^2), respectively, interacting with Val^{406} derived from chains A and C. In this mode, the turn between the α-helix and the first β-strand contains three nonidentical residues between MeuTXKα1 and BmP01 and is adjacent to the channel turret. Amino acid color codes are as follows: *blue*, basic; *green*, hydrophobic; *cyan*, polar.

provide a good example to observe how a toxin diverged after speciation by accelerated substitutions in the mature peptide-coding region. Accelerated amino acid substitutions at five sites of BmP01 and MeuTXKα1 have brought about functional diversification. First, MeuTXKα1 exhibits more potency than BmP01 on hKv1.3 (57-fold difference), and second, it is remarkable that MeuTXKα1 shows more selectivity on Kv1.3 over Kv1.1 (1271-fold difference) when compared with BmP01.

Although as naturally occurring bioactive components scorpion venom-derived KTxs have shown highly potent activity in inhibiting Kv1.3, the majority of these peptides lack sufficient specificity to distinguish between this channel and other related Kv1.x, especially Kv1.1 given the high degree of sequence similarity in the toxin-interacting pore region between Kv1.1 and Kv1.3 channels (30). For example, AgTx-2, OsK-1, NTX, and KTX bind to Kv1.3 with picomolar affinity, but their selectivity over Kv1.1 is very low, ranging from 2.6- to 110-fold (3, 31–33) (Table I). Other peptides, such as ADWX-1, HsTx1, Aam-KTX, Mokatoxin-1, and ChTX, possess high selectivity on Kv1.1, but they are also active on other related Kv

channels (*e.g.* Kv1.2) (30, 33–35). In this aspect, MeuTXKα1 has a greater advantage than the peptides mentioned above in that it works at low nanomolar concentration but displays more than 1000-fold selectivity for Kv1.3 over Kv1.1. Importantly, it lacks activity on other related Kv channels even at micromolar concentrations.

Members in the α-KTx8 subfamily have been considered as relatively weak venom components because of their overall negatively charged surfaces. The discovery of high affinity binding of MeuTXKα1 to Kv1.3 expands the pharmacological target of this unique subfamily. In fact, all the members in the α-KTx8 subfamily have two identical residues (Lys^{18} and Asn^{21}, numbered according to MeuTXKα1) that are structurally equivalent to Lys^{27} and Asn^{30} in AgTx2 and many other Kv channel-targeted α-KTxs. In AgTx2, mutations of these two key residues had the largest destabilizing effects (36). Because of the conservation in these two key residues, it is possible that MeuTXKα1 and BmP01 adopt a generally accepted mode of action to interact with Kv1.3 in which the side chain of the conserved Lys^{18} could directly plug the channel pore.

To provide structural evidence in favor of our opinion, we established a complex model of BmP01 (37) and hKv1.3 by structural superimposition and energy minimization. As shown in Fig. 11, BmP01 can well block the channel by structural complementary in which Lys^{18} enters slightly into the channel pore. This complex model allows us to recognize two hydrophobic interactions between Ala^1 (BmP01) or Val^1 (MeuTXKα1) and Val^{406} of chain A (hKv1.3) and between Pro^{28} (BmP01/MeuTXKα1) and Val^{406} of chain C (hKv1.3). Such a valine at site 406 (numbered according to hKv1.3) is only present in four sensitive Kv channels (*Shaker*, rKv1.1, rKv1.3, and hKv1.3), whereas in all resistant Kv channels, this site is replaced by Thr, Ile, or Met. A key role of this Val in AgTx2 binding to *Shaker* has been highlighted previously (36).

In our complex model, the region linking the α-helix and the first β-strand of the toxin approaches the turret, a known channel region responsible for high affinity binding of ADWX-1 to Kv1.3 (38) and AgTx2 to *Shaker* (36), which could account for the differential affinity between MeuTXKα1 and BmP01 because these two toxins have three amino acid substitutions in this region. To provide experimental evidence supporting the importance of the channel turret in interacting with the toxin, we compared the activity of BmP01 on hKv1.3 and rKv1.3, both differing by only two amino acids in the turret. The results showed that this toxin exhibited 3-fold different affinity on human and rat Kv1.3 (Fig. 9), supporting the importance of the turret of Kv1.3 in toxin binding.

In conclusion, our work, which is based on cDNA cloning and biochemical purification and functional assays, describes the molecular diversity of scorpion toxins affecting K^+ channels in a less studied species (*M. eupeus*) and functional diversification between orthologous scorpion toxins. Extremely high selectivity for Kv1.3 over Kv1.1 makes MeuTXKα1 an attractive candidate for the design of immune modulation agents for human autoimmune diseases.

Acknowledgments—We thank O. Pongs for providing the cDNA for rat Kv1.2 channel. Human Kv1.3 clone was kindly provided by M. L. Garcia. The hERG clone was generously donated by Professor Mark Keating. We also thank Dr. Rodríguez de la Vega for providing the Css20-hKv1.3 complex model.

* This work was supported by National Natural Science Foundation of China Grants 30730015 and 30921006; National Basic Research Program of China (2010CB945300) 30921006; Bilateral Cooperation for the 16th Session of the Sino-Belgian Science and Technology Mixed Commission (to S. Z.); and Fonds Wetenschappelijk Onderzoek-Vlaanderen Grants G.0330.06 and G.0257.08, Katholieke Universiteit Leuven Grant OT-05-64, Interuniversity Attraction Poles Program-Belgian State-Belgian Science Policy Grant P6/31, and BIL Grant 07/10 (China) (to J. T.).

[S] This article contains supplemental Fig. S1 and Tables S1–S3.

The nucleotide sequence(s) reported in this paper has been submitted to the GenBank™EBI Data Bank with accession number(s) EF442060, EF445085, EF442052, EF442053, EF445083, EF442047, EF445099, and EF445076.

The nucleotide sequence reported in this paper has been submitted to the Swiss Protein Database under Swiss-Prot accession no. P86400.

§ To whom correspondence should be addressed: Inst. of Zoology, Chinese Academy of Sciences, 1 Beichen West Rd., Chaoyang District, Beijing 100101, China. Tel.: 86-010-64807112; Fax: 86-010-64807099; E-mail: Zhusy@ioz.ac.cn.

REFERENCES

1. Shieh, C. C., Coghlan, M., Sullivan, J. P., and Gopalakrishnan, M. (2000) Potassium channels: molecular defects, diseases, and therapeutic opportunities. *Pharmacol. Rev.* **52,** 557–594
2. Wulff, H., Castle, N. A., and Pardo, L. A. (2009) Voltage-gated potassium channels as therapeutic targets. *Nat. Rev. Drug Discov.* **8,** 982–1001
3. Possani, L. D., Becerril, B., Delepierre, M., and Tytgat, J. (1999) Scorpion toxins specific for Na^+-channels. *Eur. J. Biochem.* **264,** 287–300
4. Tytgat, J., Chandy, K. G., Garcia, M. L., Gutman, G. A., Martin-Eauclaire, M. F., van der Walt, J. J., and Possani, L. D. (1999) A unified nomenclature for short-chain peptides isolated from scorpion venoms: alpha-KTx molecular subfamilies. *Trends Pharmacol. Sci.* **20,** 444–447
5. Gurrola, G. B., Rosati, B., Rocchetti, M., Pimienta, G., Zaza, A., Arcangeli, A., Olivotto, M., Possani, L. D., and Wanke, E. (1999) A toxin to nervous, cardiac, and endocrine ERG K^+ channels isolated from *Centruroides noxius* scorpion venom. *FASEB J.* **13,** 953–962
6. Srinivasan, K. N., Sivaraja, V., Huys, I., Sasaki, T., Cheng, B., Kumar, T. K., Sato, K., Tytgat, J., Yu, C., San, B. C., Ranganathan, S., Bowie, H. J., Kini, R. M., and Gopalakrishnakone, P. (2002) κ-Hefutoxin1, a novel toxin from the scorpion *Heterometrus fulvipes* with unique structure and function. Importance of the functional diad in potassium channel selectivity. *J. Biol. Chem.* **277,** 30040–30047
7. Bontems, F., Roumestand, C., Gilquin, B., Ménez, A., and Toma, F. (1991) Refined structure of charybdotoxin: common motifs in scorpion toxins and insect defensins. *Science* **254,** 1521–1523
8. Rodríguez de la Vega, R. C., and Possani, L. D. (2004) Current views on scorpion toxins specific for K^+-channels. *Toxicon* **43,** 865–875
9. Dauplais, M., Lecoq, A., Song, J., Cotton, J., Jamin, N., Gilquin, B., Roumestand, C., Vita, C., de Medeiros, C. L., Rowan, E. G., Harvey, A. L., and Ménez, A. (1997) On the convergent evolution of animal toxins. Conservation of a diad of functional residues in potassium channel-blocking toxins with unrelated structures. *J. Biol. Chem.* **272,** 4302–4309
10. Diego-García, E., Schwartz, E. F., D'Suze, G., González, S. A., Batista, C. V., García, B. I., de la Vega, R. C., and Possani, L. D. (2007) Wide phylogenetic distribution of Scorpine and long-chain beta-KTx-like peptides in scorpion venoms: identification of "orphan" components. *Peptides* **28,** 31–37

11. Cao, Z., Xiao, F., Peng, F., Jiang, D., Mao, X., Liu, H., Li, W., Hu, D., and Wang, T. (2003) Expression, purification and functional characterization of a recombinant scorpion venom peptide BmTXKβ. *Peptides* **24,** 187–192
12. Zhu, S., and Gao, B. (2006) Molecular characterization of a new scorpion venom lipolysis activating peptide: evidence for disulfide bridge-mediated functional switch of peptides. *FEBS Lett.* **580,** 6825–6836
13. Koradi, R., Billeter, M., and Wüthrich, K. (1996) MOLMOL: a program for display and analysis of macromolecular structures. *J. Mol. Graph.* **14,** 51–55, 29–32
14. Zhu, S., Gao, B., Aumelas, A., del Carmen Rodríguez, M., Lanz-Mendoza, H., Peigneur, S., Diego-Garcia, E., Martin-Eauclaire, M. F., Tytgat, J., and Possani, L. D. (2010) MeuTXKβ1, a scorpion venom-derived two-domain potassium channel toxin-like peptide with cytolytic activity. *Biochim. Biophys. Acta* **1804,** 872–883
15. Goudet, C., Chi, C. W., and Tytgat, J. (2002) An overview of toxins and genes from the venom of the Asian scorpion *Buthus martensi* Karsch. *Toxicon* **40,** 1239–1258
16. Liman, E. R., Tytgat, J., and Hess, P. (1992) Subunit stoichiometry of a mammalian K^+ channel determined by construction of multimeric cDNAs. *Neuron* **9,** 861–871
17. Wang, H., Zhao, L., Sun, Z., Sun, L., Zhang, B., and Zhao, Y. (2006) A potential side effect of cyclosporin A: inhibition of $CD4^+CD25^+$ regulatory T cells in mice. *Transplantation* **82,** 1484–1492
18. Corzo, G., Papp, F., Varga, Z., Barraza, O., Espino-Solis, P. G., Rodríguez de la Vega, R. C., Gaspar, R., Panyi, G., and Possani, L. D. (2008) A selective blocker of Kv1.2 and Kv1.3 potassium channels from the venom of the scorpion *Centruroides suffusus* suffusus. *Biochem. Pharmacol.* **76,** 1142–1154
19. Romi-Lebrun, R., Martin-Eauclaire, M. F., Escoubas, P., Wu, F. Q., Lebrun, B., Hisada, M., and Nakajima, T. (1997) Characterization of four toxins from *Buthus martensi* scorpion venom, which act on apamin-sensitive Ca^{2+}-activated K^+ channels. *Eur. J. Biochem.* **245,** 457–464
20. Buisine, E., Wieruszeski, J. M., Lippens, G., Wouters, D., Tartar, A., and Sautiere, P. (1997) Characterization of a new family of toxin-like peptides from the venom of the scorpion *Leiurus quinquestriatus* hebraeus. 1H-NMR structure of leiuropeptide II. *J. Pept. Res.* **49,** 545–555
21. Abdel-Mottaleb, Y., Clynen, E., Jalali, A., Bosmans, F., Vatanpour, H., Schoofs, L., and Tytgat, J. (2006) The first potassium channel toxin from the venom of the Iranian scorpion *Odonthobuthus doriae. FEBS Lett.* **580,** 6254–6258
22. Thompson, C. H., Olivetti, P. R., Fuller, M. D., Freeman, C. S., McMaster, D., French, R. J., Pohl, J., Kubanek, J., and McCarty, N. A. (2009) Isolation and characterization of a high affinity peptide inhibitor of ClC-2 chloride channels. *J. Biol. Chem.* **284,** 26051–26062
23. Gmachl, M., and Kreil, G. (1995) The precursors of the bee venom constituents apamin and MCD peptide are encoded by two genes in tandem which share the same 3′-exon. *J. Biol. Chem.* **270,** 12704–12708
24. Gauldie, J., Hanson, J. M., Rumjanek, F. D., Shipolini, R. A., and Vernon, C. A. (1976) The peptide components of bee venom. *Eur. J. Biochem.* **61,** 369–376
25. Mao, X., Cao, Z., Yin, S., Ma, Y., Wu, Y., and Li, W. (2007) Cloning and characterization of BmK86, a novel K^+-channel blocker from scorpion venom. *Biochem. Biophys. Res. Commun.* **360,** 728–734
26. Diego-García, E., Abdel-Mottaleb, Y., Schwartz, E. F., de la Vega, R. C., Tytgat, J., and Possani, L. D. (2008) Cytolytic and K^+ channel blocking activities of beta-KTx and scorpine-like peptides purified from scorpion venoms. *Cell. Mol. Life Sci.* **65,** 187–200
27. Korolkova, Y. V., Kozlov, S. A., Lipkin, A. V., Pluzhnikov, K. A., Hadley, J. K., Filippov, A. K., Brown, D. A., Angelo, K., Strøbaek, D., Jespersen, T., Olesen, S. P., Jensen, B. S., and Grishin, E. V. (2001) An ERG channel inhibitor from the scorpion *Buthus eupeus. J. Biol. Chem.* **276,** 9868–9876
28. Gao, B., Peigneur, S., Tytgat, J., and Zhu, S. (August 14, 2010) A potent potassium channel blocker from *Mesobuthus eupeus* scorpion venom. *Biochimie* 10.1016/j.biochi.2010.08.003
29. Possani, L. D., Merino, E., Corona, M., Bolivar, F., and Becerril, B. (2000) Peptides and genes coding for scorpion toxins that affect ion-channels. *Biochimie* **82,** 861–868
30. Han, S., Yi, H., Yin, S. J., Chen, Z. Y., Liu, H., Cao, Z. J., Wu, Y. L., and Li, W. X. (2008) Structural basis of a potent peptide inhibitor designed for Kv1.3 channel, a therapeutic target of autoimmune disease. *J. Biol. Chem.* **283,** 19058–19065
31. Mouhat, S., Visan, V., Ananthakrishnan, S., Wulff, H., Andreotti, N., Grissmer, S., Darbon, H., De Waard, M., and Sabatier, J. M. (2005) K^+ channel types targeted by synthetic OSK1, a toxin from *Orthochirus scrobiculosus* scorpion venom. *Biochem. J.* **385,** 95–104
32. Abdel-Mottaleb, Y., Vandendriessche, T., Clynen, E., Landuyt, B., Jalali, A., Vatanpour, H., Schoofs, L., and Tytgat, J. (2008) OdK2, a Kv1.3 channel-selective toxin from the venom of the Iranian scorpion *Odonthobuthus doriae. Toxicon* **51,** 1424–1430
33. Takacs, Z., Toups, M., Kollewe, A., Johnson, E., Cuello, L. G., Driessens, G., Biancalana, M., Koide, A., Ponte, C. G., Perozo, E., Gajewski, T. F., Suarez-Kurtz, G., Koide, S., and Goldstein, S. A. (2009) A designer ligand specific for Kv1.3 channels from a scorpion neurotoxin-based library. *Proc. Natl. Acad. Sci. U.S.A.* **106,** 22211–22216
34. Regaya, I., Beeton, C., Ferrat, G., Andreotti, N., Darbon, H., De Waard, M., and Sabatier, J. M. (2004) Evidence for domain-specific recognition of SK and Kv channels by MTX and HsTx1 scorpion toxins. *J. Biol. Chem.* **279,** 55690–55696
35. Abbas, N., Belghazi, M., Abdel-Mottaleb, Y., Tytgat, J., Bougis, P. E., and Martin-Eauclaire, M. F. (2008) A new kaliotoxin selective towards Kv1.3 and Kv1.2 but not Kv1.1 channels expressed in oocytes. *Biochem. Biophys. Res. Commun.* **376,** 525–530
36. MacKinnon, R., Cohen, S. L., Kuo, A., Lee, A., and Chait, B. T. (1998) Structural conservation in prokaryotic and eukaryotic potassium channels. *Science* **280,** 106–109
37. Wu, G., Li, Y., Wei, D., He, F., Jiang, S., Hu, G., and Wu, H. (2000) Solution structure of BmP01 from the venom of scorpion *Buthus martensii* Karsch. *Biochem. Biophys. Res. Commun.* **276,** 1148–1154
38. Yin, S. J., Jiang, L., Yi, H., Han, S., Yang, D. W., Liu, M. L., Liu, H., Cao, Z. J., Wu, Y. L., and Li, W. X. (2008) Different residues in channel turret determining the selectivity of ADWX-1 inhibitor peptide between Kv1.1 and Kv1.3 channels. *J. Proteome Res.* **7,** 4890–4897
39. Garcia, M. L., Gao, Y., McManus, O. B., and Kaczorowski, G. J. (2001) Potassium channels: from scorpion venoms to high-resolution structure. *Toxicon* **39,** 739–748
40. Possani, L. D., Selisko, B., and Gurrola, G. B. (1999) Structure and function of scorpion toxins affecting K^+-channels. *Perspect. Drug Discov. Des.* **15/16,** 15–40
41. Kharrat, R., Mabrouk, K., Crest, M., Darbon, H., Oughideni, R., Martin-Eauclaire, M. F., Jacquet, G., el Ayeb, M., Van Rietschoten, J., Rochat, H., and Sabatier, J. M. (1996) Chemical synthesis and characterization of maurotoxin, a short scorpion toxin with four disulfide bridges that acts on K^+ channels. *Eur. J. Biochem.* **242,** 491–498